Chemistry Letters

http://www.csj.jp/journals/chem-lett/

Vol.33 No.6
June, 2004

CMLTAG
ISSN 0366-7022

Highlight Review

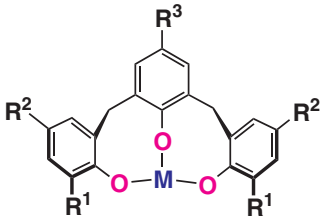

The use of covalently linked multidentate ligands is a very useful concept in coordination and organometallic chemistry. This article gives an account of the syntheses and structures of metal complexes supported by linear-linked aryloxide trimer ligands, in which aryloxide units are connected at *ortho* positions through methylene linkers.

Letter

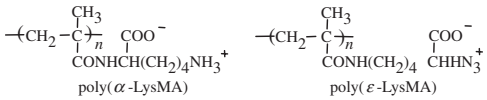

Zwitterionic polymethacrylamides, poly(N^{α}-methacrylamide-L-lysine) [poly(α-LysMA)] and poly(N^{ε}-methacrylamide-L-lysine) [poly(ε-LysMA)] were prepared to examine their bioactivity by an evaluation of fibrinolytic activity and a binding assay using resonant mirror biosensor (IAsys). Poly (α-LysMA) enhanced thefibrinolytic activity by plasminogen (Plg) / tissue-type plasminogen activator (t-PA) while no enhancement was observed in the case of poly(ε-LysMA). A strong interaction between Plg to poly(α-LysMA) was also observed by IAsys when compared with poly(ε-LysMA).

A novel visualization technique of linear dextran and dendritic amylopectin structures by means of selective deposition of an ultrathin silicate layer along sugar chains is described. This technique of "Molecular Wrapping" is also useful for visualizing an isolated cytochrome c molecule.

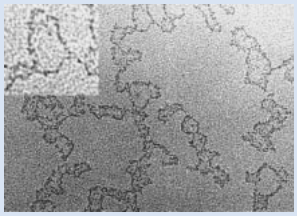

Silicate Wrapped Dextran Chain

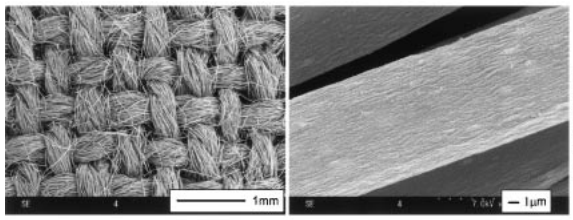

The Pt–Ru nanoporous fibres prepared using supercritical fluids exhibited a high electrocatalytic activity.

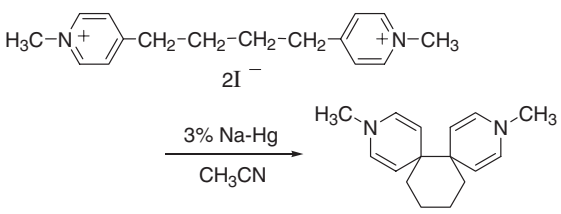

Polycrystalline CeO_2 nanowires have been synthesized via a solution-phase route using sodium bis(2-ethylhexyl) sulfosuccinate as a structure-directing agent. The obtained CeO_2 nanowires were 30–120 nm in diameters and 0.2–5 μm in lengths. The CeO_2 nanowire consists of many tiny interconnected nanocrystallites of about 7 nm in size. The Raman spectrum of CeO_2 nanowires shows size-dependent effect.

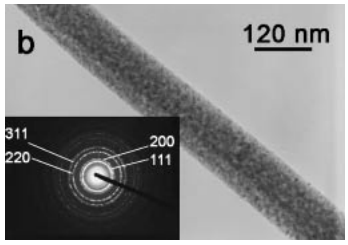

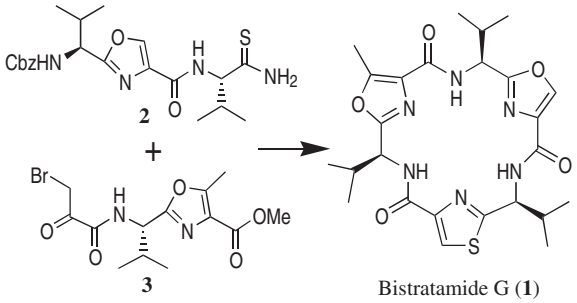

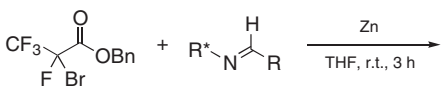

threo : *erythro* = ca. 80 : 20
>90% de for each isomer

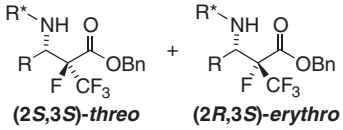

(2*S*,3*S*)-*threo* **(2*R*,3*S*)-*erythro***

668 **A New Lewis Acid System Palladium/ TMSCl for Catalytic Aldol Condensation of Aldehydes with Ketones**

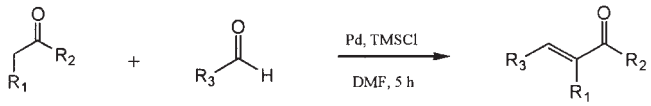

Yulin Zhu and Yuanjiang Pan

670 **A Novel Electrochemical Method for Preparation of Thin Films of Layered Manganese Oxides**

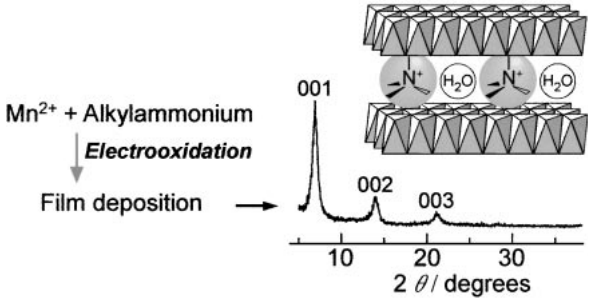

Masaharu Nakayama, Sayaka Konishi, Akihiro Tanaka, and Kotaro Ogura

672 **Controlling the Morphology and Mesostructural Orderness of the Mesoporous Silica Nanoparticles**

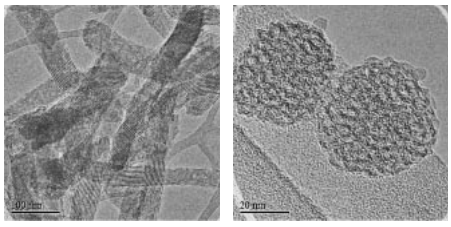

Morphology of mesoporous silica nanoparticle dependent on the pH value

Man-Chien Chao, Hong-Ping Lin, and Chung-Yuan Mou

674 **The Synthesis of 1,4-Diketones via a One-pot Five-component Connecting Reaction Based on Two Acylations of Organozincs Promoted by the Catalysis of a Pd(0) Species**

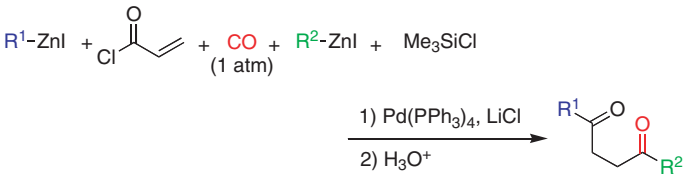

Motoki Yuguchi, Masao Tokuda, and Kazuhiko Orito

676 **Enantioselective CO_2 Fixation Catalyzed by Optically Active Cobalt Complexes**

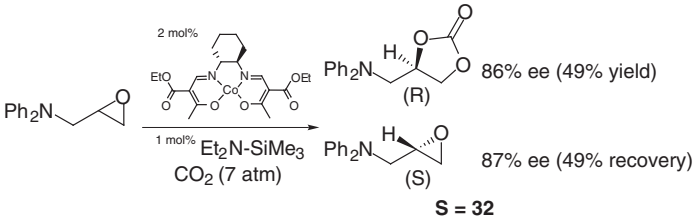

Hirotaka Tanaka, Yasunori Kitaichi, Mitsuo Sato, Taketo Ikeno, and Tohru Yamada

678 **Structure and Luminescence of a Dinuclear Copper Complex Bridged by a Diphosphine Ligand**

Taro Tsubomura, Naoki Takahashi, Ken Saito, and Toshiaki Tsukuda

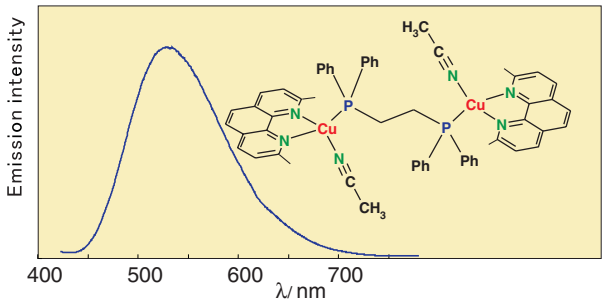

680 **Low-Viscous, Low-Melting, Hydrophobic Ionic Liquids: 1-Alkyl-3-methylimidazolium Trifluoromethyltrifluoroborate**

Zhi-Bin Zhou, Hajime Matsumoto, and Kuniaki Tatsumi

A series of new hydrophobic ionic liquids consisting of $[CF_3BF_3]^-$ anion with 1-alkyl-3-methylimidazolium cation were synthesized. All of them exhibit low viscosities (26–77 cP at 25 °C) and low melting points.

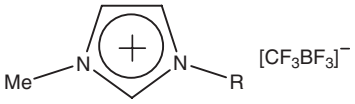

(R = methyl, ethyl, *n*-propyl, *n*-butyl, *n*-hexyl)

682 **Microbial Metabolism of Di-*n*-butyl Phthalate by Bacterium *Bacillus Natto***

Aleya Begum, Hideyuki Katsumata, Satoshi Kaneco, Tohru Suzuki, and Kiyohisa Ohta

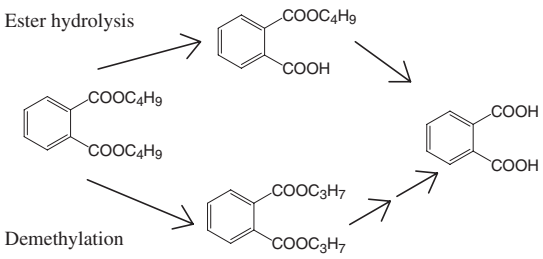

684 **Selective Binding and Cleavage of DNA by Stereoisomers of *N*,*N*′-Bis(phenanthrolin-2-yl)-1,2-cyclohexanediamine Conjugates, and Their Copper Complexes**

Keigo Hayashi, Ryouko Nakajima, Isao Kiyosawa, Hiroaki Ozaki, and Hiroaki Sawai

The DNA binding and cleaving activities of the conjugates and their copper complexes are in the order of trans- *RR* > cis > trans- *SS*.

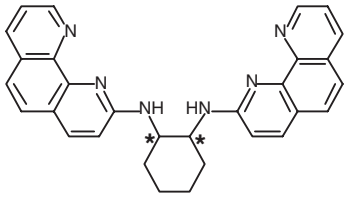

Phenanthroline-diaminocyclohexane conjugate

686 **A Medium Wherein Molecular Diffusion Takes Place the Same as in a Liquid but Convection is Prohibited**

Masao Kaneko, Norihiko Gokan, and Kiyomi Takato

Polysaccahride solid containing excess water:

Molecular diffusion takes place the same as in liqiuid but convection is prohibited

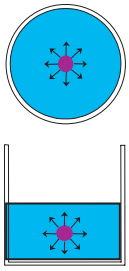

688 **Spectroelectrochemical Determination of the Redox Potential of P700 in Spinach with an Optically Transparent Thin-layer Electrode**

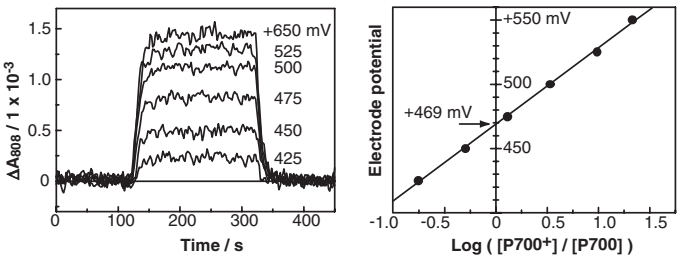

Akimasa Nakamura, Tomoyuki Suzawa, and Tadashi Watanabe

690 **Fluorescent Hydrophobic Probes Based on Intramolecular Charge Transfer State for Sensitive Protein Detection in Solution**

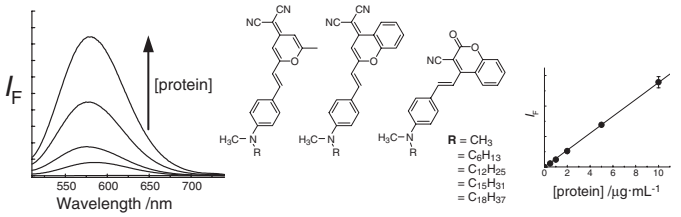

Hyunsook Jun, Soo Yeon Hong, Seung Soo Yoon, Chulhun Kang, and Myungkoo Suh

692 **Kinetic Analysis of Enzymatic Hydrolysis of Raw Starch by Glucoamylase Using an Amperometric Glucose Sensor**

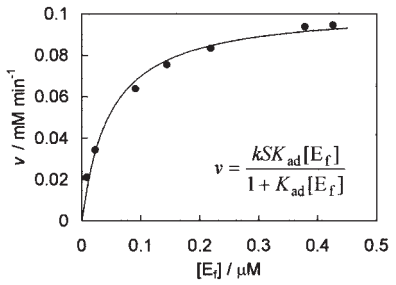

Hirosuke Tatsumi and Hajime Katano

694 **Enzymatic Synthesis of Alternatingly 6-*O*-Carboxymethylated Chitotetraose by Selective Glycosidation with Chitinase Catalysis**

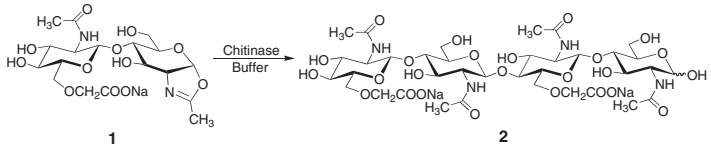

Hirofumi Ochiai, Masashi Ohmae, and Shiro Kobayashi

696 **Novel Synthesis of Disaccharides Containing the 2-Amino-2-deoxy-β-D-glucopyranosyl Unit and L-*Glycero*-D-*Manno*- and 7-Deoxy-L-*Glycero*-D-*Galacto*-heptopyranoses**

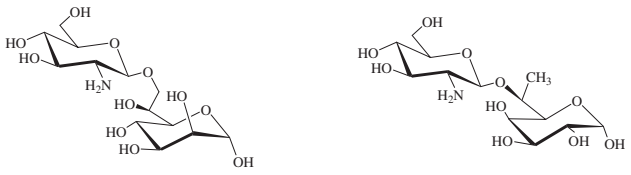

Patrick Martin, Vincent Lequart, Roméo Cecchelli, Paul Boullanger, Dominique Lafont, and Joseph Banoub

698 **Enzymatic Synthesis of 3-*O*-Methylated Chitin Oligomers from New Derivatives of a Chitobiose Oxazoline**

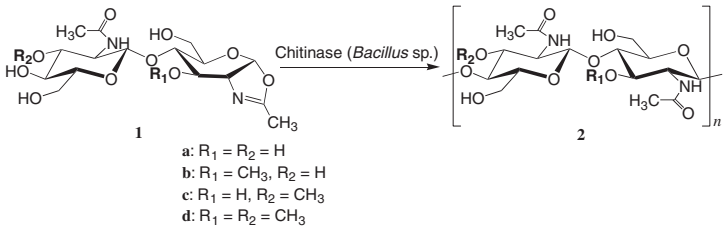

Junji Sakamoto and Shiro Kobayashi

700 **Direct Attachment of Double-stranded DNA to Gold Surface for Preparation of Nanostructured Devices**

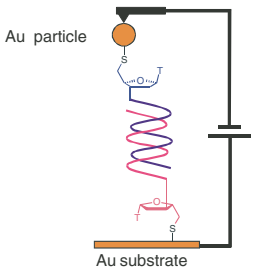

Jun Sumaoka, Fenggang Pan, Aya Nonaka, Osamu Takeuchi, Hidemi Shigekawa, and Makoto Komiyama

702 **Hg^{2+}-selective Fluorogenic Chemosensor Derived from 8-Aminoquinoline**

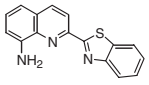

3

Compound **3** exhibited a pronounced Hg^{2+}-selective fluorescence quenching efficiency over other transition metal ions

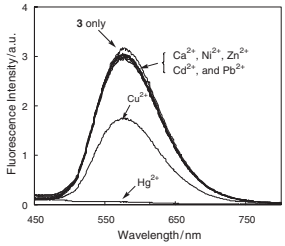

Young-Hee Kim, Jin Soo Youk, So Youn Moon, Jong-In Choe, and Suk-Kyu Chang

704 **Preparation of Layered $Li[Ni_{1/3}Mn_{1/3}Co_{1/3}]O_2$ as a Cathode for Lithium Secondary Battery by Carbonate Coprecipitation Method**

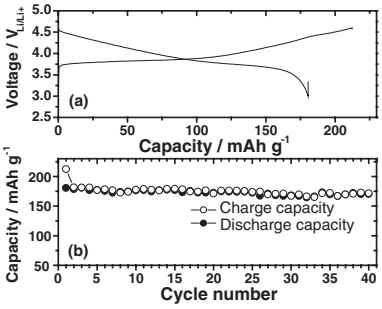

Tae-hyung Cho, Sang-mok Park, and Masaki Yoshio

706 **Novel Electron-Beam Molecular Resists with High Resolution and High Sensitivity for Nanometer Lithography**

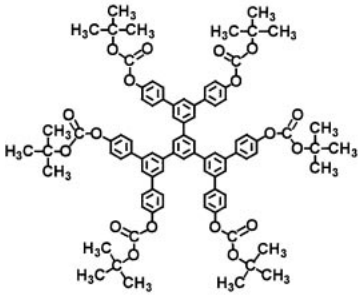

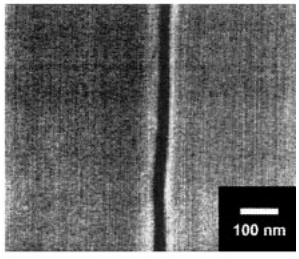

Toshiaki Kadota, Hiroshi Kageyama, Fujio Wakaya, Kenji Gamo, and Yasuhiko Shirota

708 **Hydrothermal Synthesis of Zinc Oxide Crystals in Homogeneous Mixture of Carbon Dioxide, Hydrogen, and Water**

Kiwamu Sue, Kazuhito Kimura, Kenji Murata, and Kunio Arai

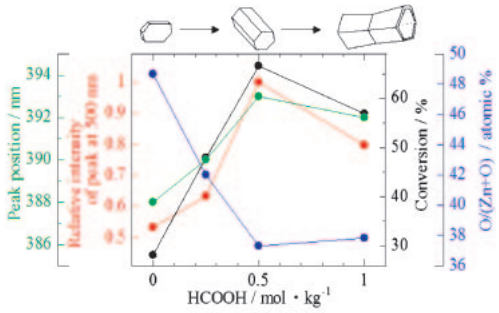

710 **Formation of a Three-Dimensional (3D) Structure of Nanoparticles Using Langmuir–Blodgett Method**

A three-dimensional nanoparticle structure was formed layer by layer by LB technique. The particles were ordered on plane and in layer by layer.

Xuehua Zhou, Chunyan Liu, Zhiying Zhang, Long Jiang, and Jinru Li

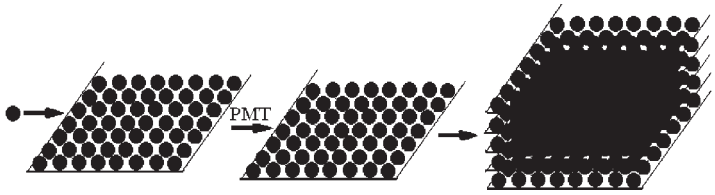

712 **Intercalation of Mercaptocarboxylic Acid into Layered Double Hydroxide Accompanied with Oxidation of Mercapto Group**

Hirokazu Nakayama, Souichiro Hirami, and Mitsutomo Tsuhako

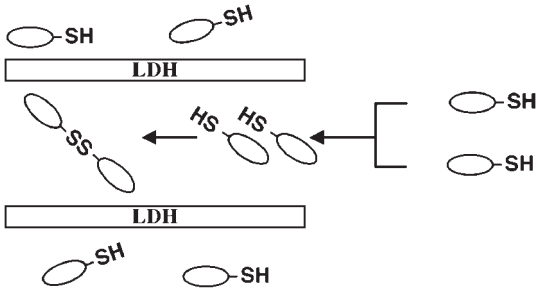

714 **Structure, Synthesis, and Biological Activity of 14-Methoxy-1,2-dehydrocacalol Methyl Ether, a New Modified Furanoeremophilane Type Sesquiterpene from *Trichilia cuneata***

Matsumi Doe, Yoshinori Hirai, Takamasa Kinoshita, Kozo Shibata, Hiroyuki Haraguchi, and Yoshiki Morimoto

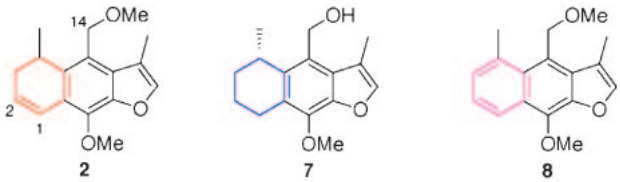

716 **9.4 T and 7.05 T Magnetic Fields Accelerate a Radical Oxidation Reaction with a Hypervalent (*tert*-Butylperoxy)iodane**

A radical oxidation of isochroman with a hypervalent iodane, 1-(*tert*-butylperoxy)-1,2-benziodoxol-3(1*H*)-one, is remarkably accelerated in 9.4 T and 7.05 T magnetic fields.

Kaori Iba, Shu-ichi Fukuyoshi, and Takenori Kusumi

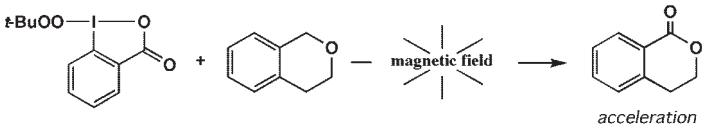

718 **Novel Lamellar Mesostructured Zinc Sulfide Nanofibers**

ZnS nanofibers were prepared via a simple hydrothermal route using alkylamines as structure-directing template and EDTA as stabilizer. The obtained ZnS nanofibers adopt lamellar mesostructure and the distance between the layers can be adjusted simply by changing the length of the alkylamine.

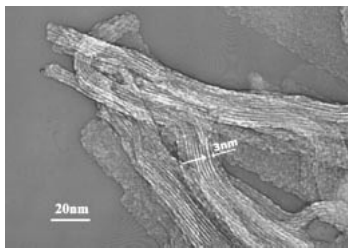

Junping Li, Yao Xu, Dong Wu, and Yuhan Sun

720 **Controllable Morphology Formation of Gold Nano- and Micro-plates in Amphiphilic Block Copolymer-based Liquid Crystalline Phase**

Luyan Wang, Xiao Chen, Jie Zhan, Zhenming Sui, Jikuan Zhao, and Zhenwen Sun

722 **A Step-Growth Model for Molecular Mechanisms of Monolayer Formation in Ordered Nanoporous Channels**

Ordered nanoporosity provides a unique environment to assemble functional nanoscale materials. The surface roughness on the nanometer and subnanolevel has large implications on how the molecules assemble in the pore channels.

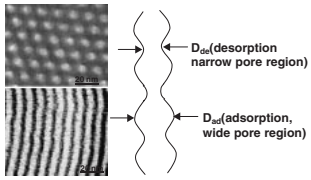

Jeong Ho Chang, Chang Han Shim, Kyung Ja Kim, and Jun Liu

724 **Formation of 10 nm-sized Oxo(phtalocyaninato)vanadium(IV) Particles by Femtosecond Laser Ablation in Water**

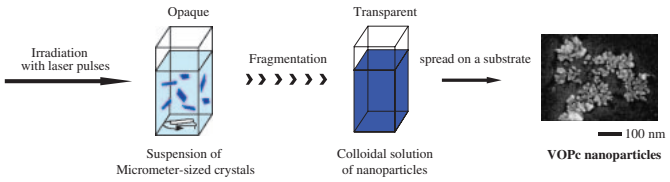

Teruki Sugiyama, Tsuyoshi Asahi, and Hiroshi Masuhara

726 **Photocatalytic Decomposition of H_2O into H_2 and O_2 over Ga_2O_3 Loaded with NiO**

Photocatalytic decomposition of H_2O into H_2 and O_2 over NiO-loaded Ga_2O_3, one of the oxides with a d^{10} electron configuration, was confirmed.

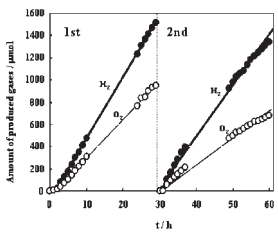

Takashi Yanagida, Yoshihisa Sakata, and Hayao Imamura

728 **Novel Dimerization, Alkoxylation, and Sulfidation of Olefins Catalyzed by $RuCl_3 \cdot nH_2O$**

Mitsuteru Higashimura, Keita Imamura, Yukiko Yokogawa, and Tsutomu Sakakibara

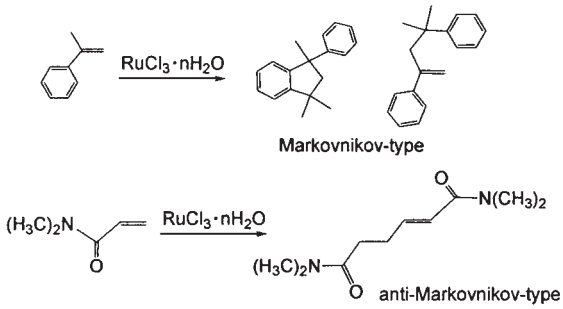

730 **Codoped Rutile TiO_2 as a New Photocatalyst for Visible Light Irradiation**

(S, La_2O_3)-codoped rutile TiO_2 by hydrothermal treated at 200 °C for 2 h has efficient photocatalytic activities for degradation of methylene blue (MB) under the visible light irradiation. Although the codoping quantity was small, the codoping of S and La_2O_3 made the degradation rate of MB as high as 98.4%.

Hongyan Liu and Lian Gao

732 **Fabrication and Degradation of Polyperoxides by a Radical Chain Process under Mild Conditions**

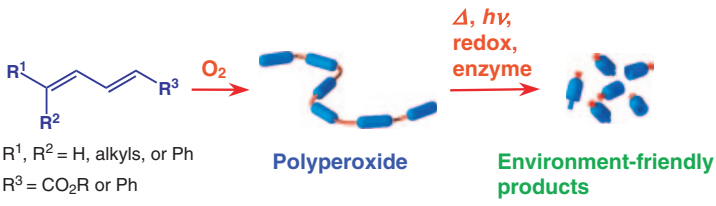

Akikazu Matsumoto and Shuji Taketani

734 **Determination of Silica Mesophases by Controlling Silicate Condensation in Liquid Phase**

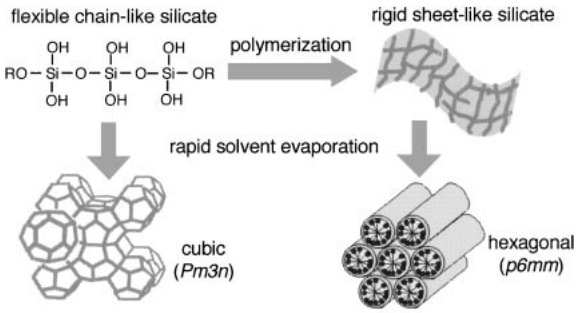

Masaru Ogura, Yushi Suzuki, Hayato Miyoshi, Sajo P. Naik, and Tatsuya Okubo

736 **Efficient Photocatalytic Oxidation of Cycloalkenes by Dihydroxo(tetraphenylporphyrinato)antimony Supported on Silica Gel under Visible Light Irradiation**

Silica gel-supported dihydroxo(tetraphenylporphyrinato)antimony (V) complex, $[SbTPP(OH)_2]^+/SiO_2$, operated as a photocatalyst under visible-light irradiation. The irradiation $[SbTPP(OH)_2]^+/SiO_2$ particles with cycloalkenes by fluorescent light gave mainly cycloalkene oxide and 2-cycloalken-1-ol.

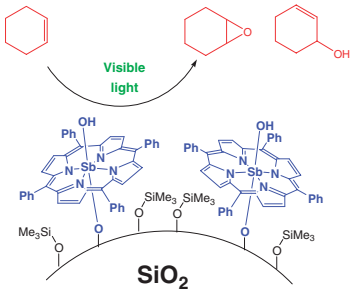

Tsutomu Shiragami, Ryu-ichi Makise, Yousuke Inokuchi, Jin Matsumoto, Haruo Inoue, and Masahide Yasuda

738 **Preparation of Porous SnO_2 Particles Having High Specific Surface Area and High Thermal Stability via an Aqueous Solution Route and Subsequent Hydrothermal Treatment**

Hierarchically tailored SnO_2 particles with a diameter of 200–500 nm were grown in aqueous solutions dissolving SnF_2 at 60 °C. The porous architecture of the particles was composed of SnO_2 crystallites of ca. 5 nm in diameter and exhibited a high specific surface area in the range between 130 and 230 m^2/g. Subsequent hydrothermal treatment at 150 °C increased the crystallinity with removal of fluorine from the surface and improved the thermal stability of the SnO_2 fine structure.

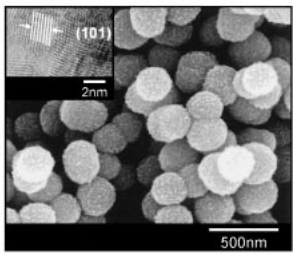

Hirotoshi Ohgi, Takahiro Maeda, Shinobu Fujihara, and Hiroaki Imai

740 **Bioinspired Modification of Polystyryl Matrix: Single-step Chemical Evolution to a Moderately Conducting Polymer**

In a bioinspired approach, moderate conduction in otherwise insulating polystyrene (**PS**) has been engineered by the sheer introduction of adenine nucleobases.

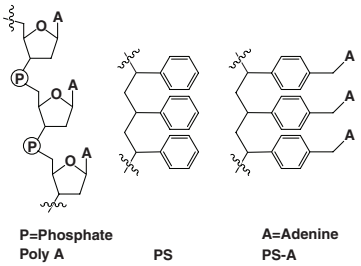

Ashutosh Saxena, S. G. Srivatsan, Vishal Saxena, and Sandeep Verma

742 **Synthesis of *N*,*N*′-Disubstituted Urea from Ethylene Carbonate and Amine Using CaO**

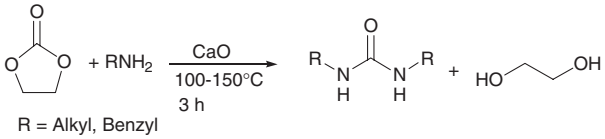

Shin-ichiro Fujita, Bhalchandra M. Bhanage, and Masahiko Arai

744 **Novel Plasma Methanol Decomposition to Hydrogen Using Corona Discharges**

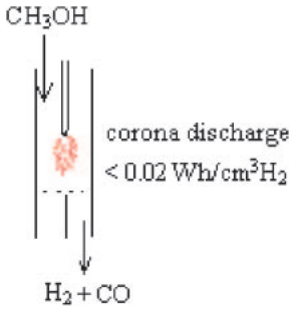

Hui-qing Li, Ji-jun Zou, Yue-ping Zhang, and Chang-jun Liu

746 **Growth of Trigonal-shaped TiN Nanocrystals via the Metal-catalyzed Reduction-Nitridation Route at Low Temperature**

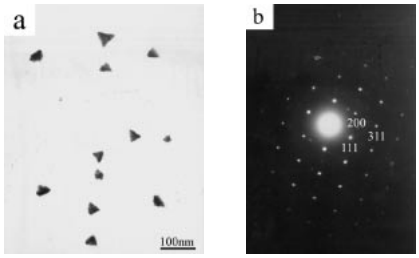

(a) TEM image of the trigonal-shaped TiN nanocrystalline;
(b) The corresponding selected-area electron pattern (SAED).

Xuchu Ma, Zude Zhang, Xuebing Li, Shutao Wang, Yi Du, Fen Xu, and Yitai Qian

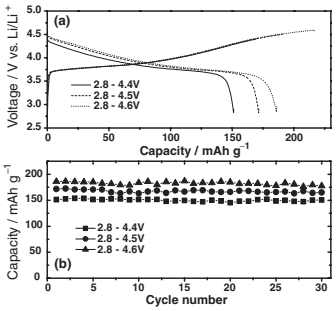

Absorption spectra of carbonate species-doped TiO_2 and pure TiO_2 (ST-01:anatase) photocatalysts

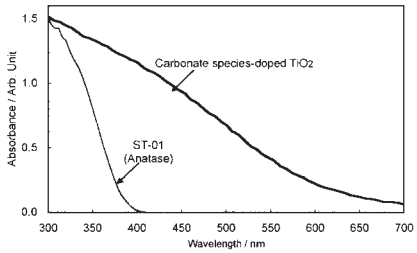

Mutations at a well-conserved Arg410 located near the heme proximal axial ligand in the oxygenase domain of neuronal NOS (nNOS) abolished both substrate recognition and electron transfer to the heme, suggesting that this residue plays an important role in the architecture of the substrate recognition site and the electron transfer process.

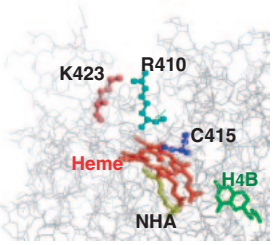

Ag_2S nanorods were synthesized via a solution-phase ion-exchange route at room temperature.

Charge-transfer complexes of **1** and TCNE are affected by π–π interaction and NH–π interaction.

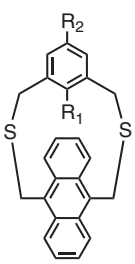

1a:R_1=R_2=H
1b:R_1=OMe, R_2=*t*-Bu
1c:R_1=NO_2, R_2=H
1d:R_1=H, R_2=NO_2
1e:R_1=NH_2, R_2=H
1f:R_1=H, R_2=NH_2

758 **Theoretical Design of a New Optical Durable Molecular Switch**

A new inorganic molecule that can be used as a new optical durable molecular switch was theoretically designed in the framework of density functional theory. Two energy minima were found in the molecule, and their electronic states were low-spin ^1A_g and high-spin $^5A_1$, respectively. The predicted infrared spectra in each state showed that the new inorganic molecule have quite different spectra patterns. This means that the molecule can be used as an optical durable molecular switch.

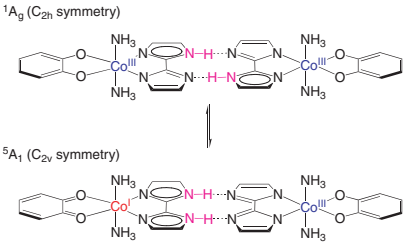

Hirotoshi Mori and Eisaku Miyoshi

760 **Tellurium Nanorods and Nanowires Prepared by the Microwave-Polyol Method**

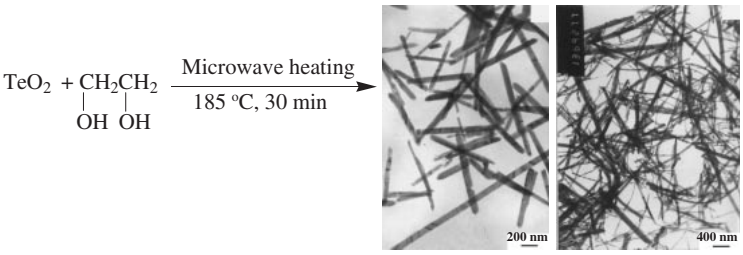

Ying-Jie Zhu and Xian-Luo Hu

762 **Fiber-optic Detection of DNA Denaturation for SNP Analysis**

The difference in melting temperature (Tm) between perfectly and SNP-matched probe-target hybrids is determined with fiber-optic detection system by derivative analysis of the melting curves.

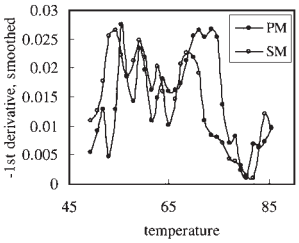

Kaori Honda, Yasumitsu Kondoh, Tokuji Kitsunai, Katsuo Nishi, and Hideo Tashiro

764 **Palladium-catalyzed Stereospecific Epoxide-opening Reaction of γ,δ-Epoxy-α,β-unsaturated Esters with Boric Acid Leading to γ,δ-Diol Derivatives with Double Inversion of Configuration**

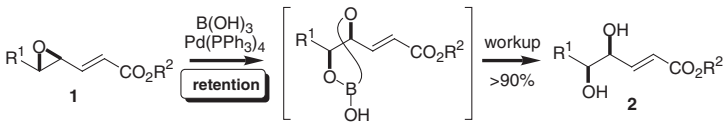

Xiao-Qiang Yu, Atsushi Hirai, and Masaaki Miyashita

766 **Preparation and Characterization of Tungsten-substituted Molybdenum Disulfide Nanorods**

The tungsten-substituted molybdenum disulfide nanorods were synthesized by thermal decomposition of the corresponding trisulfide precursor that was prepared in reversed micelles.

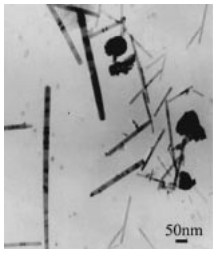

Junbao Xia, Zhude Xu, Weixiang Chen, Qiulin Nie, and Guohua Li

768 **Phosphate-mediated ZnO Nanosheets with a Mosaic Structure**

Hiroaki Imai, Satoko Iwai, and Satoshi Yamabi

Seaweed-like ZnO sheets consisting of wurtzite-type nanoplates with a thickness less than 5 nm were grown in an aqueous solution system containing phosphate anions. The platy crystals were formed with specific adsorption of phosphate anions on the (001) plane.

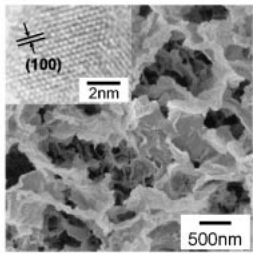

770 **A New Reaction to ZnO Nanoparticles**

Hongchu Du, Fangli Yuan, Shulan Huang, Jinlin Li, and Yongfa Zhu

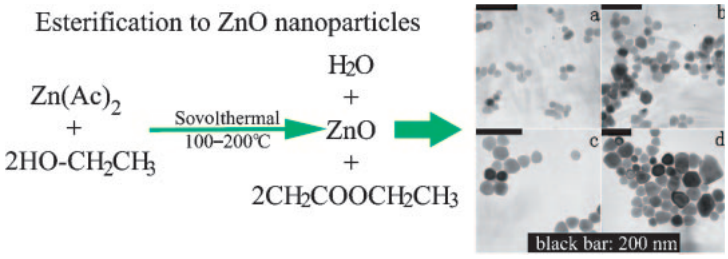

772 **Self-assembled Monolayer of Light-harvesting 1 and Reaction Center (LH1-RC) Complexes Isolated from *Rhodospirillum rubrum* on an Amino-Terminated ITO Electrode**

Makiko Ogawa, Kiyoshi Shinohara, Yukari Nakamura, Yoshiharu Suemori, Morio Nagata, Kouji Iida, Alastair T. Gardiner, Richard J. Cogdell, and Mamoru Nango

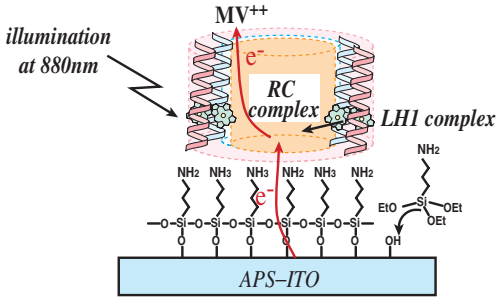

774 **Synthesis of Hexagonal Mesostructured $FePO_4$ Using Cationic Surfactant as the Template**

Shenmin Zhu, Haoshen Zhou, Mitsuhiro Hibino, and Itaru Honma

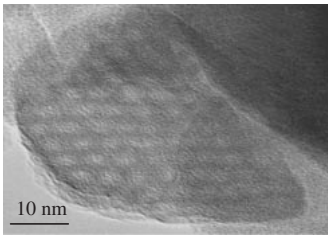

Highly-ordered hexagonally mesostructured iron phosphate was reported for the first time to be synthesized by an effective, fast, easy approach using cationic surfactant as the template.

776 **Hybrid Reagent of Ammonium Hydrogen Fluoride and Scandium Triflate: Highly Efficient Catalyst for Ring-opening Fluorination of 2,3-Epoxyalcohols**

Yoshimitsu Itoh, Sejin Jang, Siho Ohba, and Koichi Mikami